Measurements of Effective Self-diffusion Coefficients in a Gel-Type Cation Exchanger by the Zero-Length-Column Method

Juan F. Rodríguez,[†] Jose L. Valverde,[†] and Alirio E. Rodrigues*[,‡]

Department of Chemical Engineering, Faculty of Chemistry, University of Castilla−La Mancha, Campus Universitario s/n, 13004 Ciudad Real, Spain, and Laboratory of Separation and Reaction Engineering, Faculty of Engineering, University of Porto, 4099 Porto Codex, Porto, Portugal

The zero-length column (ZLC), conventionally developed for measuring the diffusivity of gases and liquids in zeolite crystals, has been extended to the measurement of intraparticle diffusivities in ion exchangers. A theoretical model which considers the ZLC cell as a continuous stirred tank reactor is developed. The model allows the use of nonlinear ion-exchange equilibrium isotherms, describes ion fluxes with Nernst−Planck equations, and includes the resistances to mass transfer both in the particle and in the film. Simulations have been carried out to analyze the effect of model parameters on the system response and to choose experimental operating conditions. The model validity has been tested by comparison with the experimental results of the ZLC for a step perturbation in the binary systems Na^+-H^+, K^+-H^+, and Na^+-K^+.

Introduction

The zero-length-column (ZLC) method, introduced by Eic and Ruthven (1988), has been shown to provide a simple and relatively straightforward technique of measuring diffusion coefficients in zeolite particles. This method has been widely applied to gaseous (Brandani and Ruthven, 1996; Silva and Rodrigues, 1997) and liquid systems (Ruthven and Stapleton, 1993; Brandani and Ruthven, 1995).

Batch, shallow bed, or single-particle methods have been applied for the measurement of intraparticle diffusivities in ion exchangers. Essentially, the ZLC technique differs from the shallow bed technique, used for the measurement of film mass transfer at low flow rates, because it is operated in the other extreme region (high flow rate, negligible film mass-transfer resistance). On the other hand, ZLC behaves as a continuous-stirring tank adsorber where the concentration at the pellet surface is related to the outlet concentration of the ZLC. The boundary condition at the pellet surface in a ZLC is slightly modified compared with the finite bath problem (Silva and Rodrigues, 1997).

The ZLC is a differential bed of resin particles which is primarily saturated with a solution of ions. At zero time a solution containing a different counterion is fed at sufficiently high flow rate and the desorption curve is analyzed in terms of the concentration of the ion initially present in the resin phase as a function of time. Once the resin is completely saturated with the entering counterion, the reverse elution operation can be carried out, returning the resin sample to the primitive state.

Different approaches for modeling the kinetics of ion-exchange processes have been used. The resin particles can be described as porous or gel particles where only a quasi-homogeneous phase exists. A pore diffusion model might be employed in the first case, while a homogeneous model would represent better the physical reality in the second (Helfferich, 1990).

Ion fluxes can be described either by the Fick approximation or by the Nernst−Planck approximation. In any case, one has to consider the homogeneous or the macroporous nature of the particle, to obtain a reasonable description of the diffusional process. The Nernst−Planck (NP) model accounts for the influence of the electric field caused by the differences in the mobilities of counterions on the ion-exchange rate, while Fick's law considers only diffusion. Differences between uptake and elution kinetics for a given system and the dependence of the exchange rate with the concentration of each counterion can be only predicted by the NP model (Chowdiah and Foutch, 1995). However, in binary ion exchange it is possible to use model equivalence between NP and Fick's models and use the simplified Fick's law with a corrected diffusion coefficient to describe ion-exchange processes (Rendueles de la Vega et al., 1996).

External mass-transfer resistance also affects the ion-exchange rate. In general, at low solution concentrations external mass transfer is dominant, while intraparticle diffusional resistance is normally dominant at higher solution concentrations. It is generally accepted that, below a value of 0.1 mol/L, film diffusion is able to be the controlling mechanism (Kraaijeveld and Wesselingh, 1993).

The objectives of this work are as follows:

(i) To develop a mathematical model to describe the response of the ZLC ion-exchange system. The model includes the resistance to mass transfer in the film and inside the particle, a constant separation factor to describe the ion-exchange equilibrium at the particle surface, and the effect of the electric field.

(ii) To analyze the effect of the model parameters on the response curves and choose the operating conditions needed to measure intraparticle diffusivities of ions.

(iii) To test the model validity in various ion-exchange systems: Na^+-H^+, K^+-H^+, and K^+-Na^+.

* To whom correspondence should be addressed. E-mail: arodrig@fe.up.pt. Telephone: 351 2 2041671. Fax: 351 2 2041674.

[†] University of Castilla−La Mancha.

[‡] University of Porto.

S0888-5885(97)00684-2 CCC: $15.00
Published on Web 04/17/1998

Mathematical Model

The resin used in the present work is a gel-type resin. Thus, the homogeneous model will represent better the physical reality inside the particle.

Model equations have been derived under the following simplifying assumptions:

(i) The whole resin is treated as a quasi-homogeneous phase. Resin beads are assumed to be completely spherical in shape with no appreciable volume changes during the ion-exchange process.

(ii) The effects of pressure gradients and activity coefficients are neglected.

(iii) Co-ion concentration in the ion exchanger is negligible.

(iv) Ion intraparticle diffusivities do not depend on particle concentration.

Considering an ion-exchange isothermal process between an ion i presaturating the resin and an ion j entering the resin particle,

$$\overline{\mathrm{R}^{-}{}^{+}i} + j^{+} \Leftrightarrow \overline{\mathrm{R}^{-}{}^{+}j} + i^{+} \tag{1}$$

the Nernst−Planck equations for the ionic flux of counterions i and j are respectively

$$N_i = -D_i \frac{\partial q_i}{\partial r} - D_i z_i q_i \frac{F}{RT} \frac{\partial \phi}{\partial r} \tag{2a}$$

$$N_j = -D_j \frac{\partial q_j}{\partial r} - D_j z_j q_j \frac{F}{RT} \frac{\partial \phi}{\partial r} \tag{2b}$$

where q is the resin phase concentration, D is the effective diffusivity of the ion, z is the electrochemical valence, r is the space coordinate in the particle assumed with spherical geometry, ϕ is the electric potential, F is the Faraday constant, R is the perfect gas constant, and T is the temperature. Assuming that no electric current develops and that there are no vacant ionic sites inside the resin, i.e., that the electroneutrality condition is verified, the model includes the following equations:

$$z_i N_i + z_j N_j = 0 \tag{3}$$

$$z_i q_i + z_j q_j = Q \tag{4}$$

Only the case of equal valence ions, namely, monovalent ions, will be considered; in this case $N_i + N_j = 0$. The term corresponding to the electric field in eq 2a,b can be eliminated, so

$$\frac{F}{RT} \frac{\partial \phi}{\partial r} = \frac{D_j - D_i}{[q_i(D_i - D_j) + QD_j]} \frac{\partial q_i}{\partial r} \tag{5}$$

The general equation corresponding to the flux of ion i, expressed in terms of the concentration gradient, is then

$$N_i = -D_i \left[1 + \frac{q_i(1-\delta)}{Q + q_i(\delta - 1)}\right] \frac{\partial q_i}{\partial r} \tag{6}$$

where $\delta = D_i/D_j$ is the ratio between the diffusivities of species i and j and D_{ij} is the interdiffusion coefficient

$$D_{ij} = D_i \left[1 + \frac{q_i(1-\delta)}{Q + q_i(\delta - 1)}\right] \tag{7}$$

The mass balance in the resin particle is

$$\frac{\partial q_i}{\partial t} = -\frac{1}{r^2} \frac{\partial (r^2 N_i)}{\partial r} \tag{8}$$

and introducing the flux equation (6), we get

$$\frac{\partial q_i}{\partial t} = \frac{2D_i Q}{r(Q + (\delta - 1)q_i)} \left(\frac{\partial q_i}{\partial r}\right) + \frac{D_i Q(\delta - 1)}{(Q + (\delta - 1)q_i)^2} \left(\frac{\partial q_i}{\partial r}\right)^2 + \frac{D_i Q}{(Q + (\delta - 1)q_i)} \left(\frac{\partial^2 q_i}{\partial r^2}\right) \tag{9}$$

with initial and boundary conditions

$$t = 0: \qquad q_i = Q \qquad C_i = C_{i_0} = C_{\mathrm{T}} \tag{10}$$

$$r = 0: \qquad \frac{\partial q_i}{\partial r} = 0 \tag{11}$$

and taking into account the resistance in the film to mass transfer,

$$r = R_{\mathrm{p}}: \qquad -D_{ij} \left.\frac{\partial q_i}{\partial r}\right|_{r=R_{\mathrm{p}}} = K_{\mathrm{L}}(C_i^{\mathrm{s}} - C_i) \tag{12}$$

where the concentration at the solid resin surface q_i^{s} is related to the concentration of the liquid C_i^{s} by an equilibrium relation based on the mass action law:

$$q_i^{\mathrm{s}} = \frac{QC_i^{\mathrm{s}}}{KC_{\mathrm{T}} + (1 - K)C_i^{\mathrm{s}}} \tag{13}$$

The mass balance for the ZLC is

$$V(1-\epsilon) \frac{\mathrm{d}\overline{q_i}}{\mathrm{d}t} + V\epsilon \frac{\mathrm{d}C_i}{\mathrm{d}t} + FC_i = 0 \tag{14}$$

where

$$\frac{\mathrm{d}\overline{q_i}}{\mathrm{d}t} = 3\frac{D_{ij}}{R_{\mathrm{p}}} \left.\frac{\partial q_i}{\partial r}\right|_{r=R_{\mathrm{p}}} \tag{15}$$

In the above equation $\overline{q_i}$ is the average species concentration in the resin phase.

Introducing the following dimensionless variables

$$Y_i = \frac{q_i}{Q}; \qquad X_i = \frac{C_i}{C_{\mathrm{T}}}; \qquad \tau = \frac{D_i t}{R_{\mathrm{p}}{}^2}; \qquad R = \frac{r}{R_{\mathrm{p}}} \tag{16}$$

Equation 9 becomes:

$$\frac{\partial Y_i}{\partial \tau} = \frac{2}{R(1 + (\delta - 1)Y_i)} \left(\frac{\partial Y_i}{\partial R}\right) + \frac{(\delta - 1)}{(1 + (\delta - 1)Y_i)^2} \left(\frac{\partial Y_i}{\partial R}\right)^2 + \frac{1}{(1 + (\delta - 1)Y_i)} \left(\frac{\partial^2 Y_i}{\partial R^2}\right) \tag{17}$$

The initial and boundary conditions in dimensionless

form are respectively

$$\tau = 0: \qquad Y_i = 1 \qquad X_i = 1 \tag{18}$$

$$R = 0: \qquad \frac{\partial Y_i}{\partial R} = 0 \tag{19}$$

$$R = 1: \ \frac{C_{si}}{(1 + (\delta - 1)Y_i)} \frac{\partial Y_i}{\partial R}\bigg|_{R=1} = \frac{1 - \epsilon}{\epsilon} Nu(X_i - X_i^s) \tag{20}$$

with the equilibrium relation

$$Y_i^s = \frac{X_i^s}{K + (1 - K)X_i^s} \tag{21}$$

where

$$C_{si} = \frac{Q(1 - \epsilon)}{C_T \epsilon} \qquad \text{(capacity factor)} \tag{22a}$$

$$Nu = \frac{K_L R_p}{D_i} \qquad \text{(Nusselt number)} \tag{22b}$$

The ZLC mass balance in dimensionless form

$$\frac{3C_{si}}{(1 + (\delta - 1)Y_i)} \frac{d\bar{Y}_i}{d\tau} + \frac{dX_i}{d\tau} + LX_i = 0 \tag{23}$$

where

$$L = \frac{FR_p^2}{V\epsilon D_i} = \frac{\text{time constant for diffusion}}{\text{space time}} \tag{24}$$

$$\frac{d\bar{Y}_i}{d\tau} = \frac{3}{(1 + (\delta - 1)Y_i)} \frac{\partial Y_i}{\partial R}\bigg|_{R=1} \tag{25}$$

Model parameters are as follows:

(i) Equilibrium parameters: K and $C_{si} = Q(1 - \epsilon)/C_T\epsilon$.

(ii) Diffusivity ratio: $\delta = D_i/D_j$.

(iii) Nusselt number: $Nu = K_L R_p/D_i$.

(iv) ZLC parameter: $L = FR_p^2/V\epsilon D_i$.

The above system of equations has been solved by using orthogonal collocation on finite elements with Lagrange cubic polynomials as trial functions (Finlayson, 1980). Five finite elements with two interior collocation points were used to solve the theoretical equations. In this way, the partial differential equations (17) and (25) are transformed into ordinary differential equations. The resulting initial value problem in time is then numerically solved by using a predictor−corrector procedure. At a new time, one has values of the solution at each interior collocation point. However, the values of the dimensionless particle concentration at $R = 0$ and $R = 1$ and at the points between elements remain unknown. These values can be obtained by solving the nonlinear algebraic equations constituted by the two boundary conditions and the continuity of flux between elements. For that purpose, Marquardt's algorithm has been used (Marquardt, 1963).

Simulation Results

The available ZLC models for desorption of solutes in liquid systems would find applicability for counterions with the same mobility, $\delta = 1$ and $K = 1$, namely, in isotopic ion exchange, where the process could be represented as a simple Fickian diffusional process (Brandani and Ruthven, 1995).

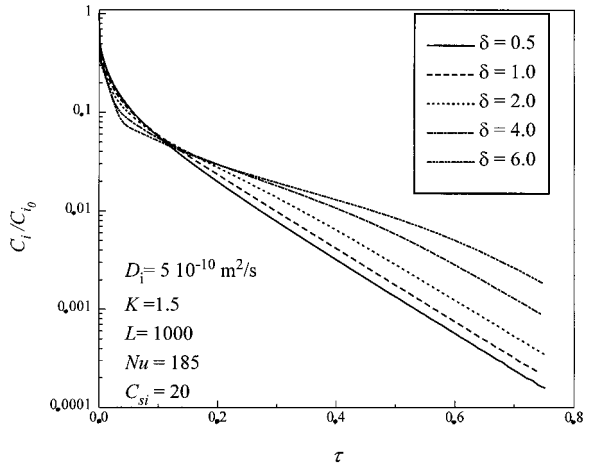

Figure 1. Theoretical desorption curves, C_i/C_{i_0} vs τ, calculated from the ZLC model. Influence of the diffusivity ratio of the counterions, δ. ($D_i = 5 \times 10^{-10}$ m^2/s, $K = 1.5$, $L = 1000$, $Nu = 185$, $C_{si} = 20$.)

However, when ions with different mobilities are involved in the process, it will be necessary to take into account Nernst−Planck equations. Figure 1 shows the desorption curves for different values of the relation between the diffusion coefficients, $\delta = D_i/D_j$, at fixed and realistic values of all other parameters. Only when $\delta = 1$ does the desorption curve approximate a straight line at long time. This behavior is the same as is observed when a single solute is desorbed from an adsorbent in gaseous or liquid ZLC systems.

The initial part of the response curves corresponds with the washing up of the cell. Following the minority rule, the exchange rate in that initial part of the elution process is limited by the diffusivity of the entering ion. Accordingly, as the diffusivity of the entering ion increases, the flux of the ion initially in the resin grows. One can observe that the concentration of the eluted ion in the effluent diminishes more slowly during the washing up part when the diffusivity of the entering ion is large. On the contrary, when the diffusivity of the entering ion is low, the ion initially in the resin is more slowly exchanged; then the solution of the cell is rapidly washed up, and the concentration decreases more sharply. The final part of all these parametric elution curves tends to straight parallel lines. In that part, the process is controlled by the self-diffusion coefficient of the minority ion, the one initially in the resin, which is the same for all the parametric curves.

This effect is only seen when the Nernst−Planck model is used. Other important conclusions may be drawn from Figure 1; the ion-exchange cycle of exchange elution must be necessarily asymmetrical for the reversal elution of each counterion since the values of δ and K are reciprocals of those in the previous step.

Figure 2 shows the effect of the equilibrium constant on the response curves for a fixed set of parameters. As expected, the response of the system agrees with the response that can be obtained from a perfectly mixed sorber for a step change of concentration at inlet for different K values (Rodrigues and Beira, 1979). The process can be equilibrium controlled when the isotherm is very unfavorable $K < 0.1$, being difficult to say

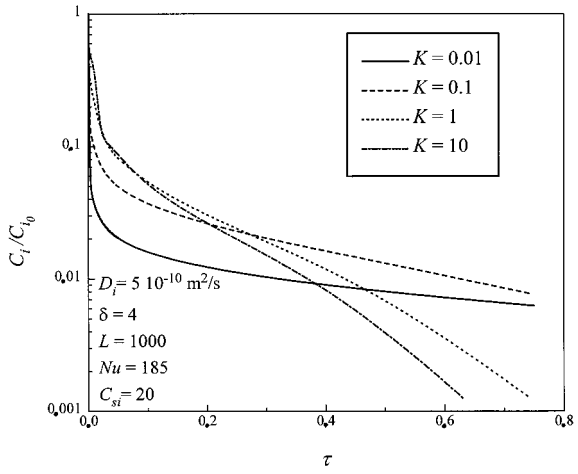

Figure 2. Theoretical desorption curves, C_i/C_{i_0} vs τ, calculated from the ZLC model. Influence of the equilibrium constant, K. ($D_i = 5 \times 10^{-10}$ m^2/s, $\delta = 4$, $L = 1000$, $Nu = 185$, $C_{si} = 20$.)

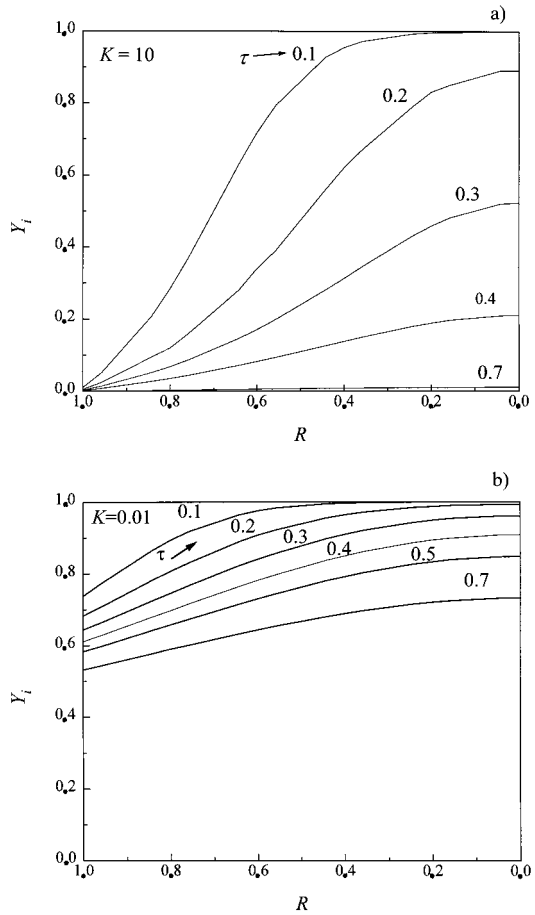

Figure 3. Evolution of the dimensionless radial concentration profiles, Y_i vs R, inside the particle calculated from the ZLC model. Influence of the separation factor: (a) $K = 0.01$, (b) $K = 10$. ($D_i = 5 \times 10^{-10}$ m^2/s, $\delta = 4$, $L = 1000$, $Nu = 185$, $C_{si} = 20$.)

nothing about the diffusion coefficients in such conditions. As can be seen in Figure 3, for identical operating conditions the evolution of the dimensionless profiles inside the particle is very different for different K values. When $K = 0.01$, the greater affinity of the resin by the sorbed ion produces nearly flat concentration profiles inside the particle, namely, the process is then exclusively controlled by the equilibrium relation. Nevertheless, for almost all the practical situations in ion exchange ($0.1 < K < 10$), that technique can offer valuable and reliable information about the system.

On the other hand, the distribution coefficient K has a strong influence on the shape of the first part of the elution curve, the washing up zone. The slope of the curve in the initial part increases as the distribution coefficient decreases, namely, for unfavorable isotherms. For a favorable isotherm, the resin prefers the ion in solution and the adsorbed one is easily and rapidly released. Then, the concentration of the eluted ion in the effluent diminishes more slowly. On the contrary, for a system with an unfavorable isotherm the ion exchanger prefers the ion initially in the resin, which is more slowly exchanged in which the solution of the cell is rapidly washed up and the concentration decreases very sharply.

The parameters δ and K are related to the physical and chemical properties of the species, and they cannot be varied for a given system. L and Nu are the dynamic parameters of the system, and C_{si} is the capacity parameter. They include variables that can be easily modified in order to reach a different controlling mechanism. While C_{si} can be varied independently, a change in the value of L also changes Nu because the value of the external mass-transfer coefficient K_L is related to the conditions in the ZLC, especially with the flow rate and the resin particle size.

To describe the mass transfer through the external film, the following relation (Kataoka et al., 1973) was employed:

$$\frac{K_L \epsilon_b}{u} = 1.85 Re^{-2/3} Sc^{-2/3} \left(\frac{1-\epsilon_b}{\epsilon_b}\right)^{-1/3} \qquad (26)$$

where u is the superficial velocity and Sc is the Schmidt number and Re is the Reynolds number defined as

$$Sc = \frac{\mu}{\rho D^f} \quad \text{and} \quad Re = \frac{\rho(2R_p u)}{\mu(1-\epsilon_b)} \qquad (27)$$

where μ and ρ are the viscosity and the density of the solution, respectively, and ϵ_b is the porosity of the resin bed. D^f is the free solution diffusivity of the entering ion, i.e., the minority ion in the film at the beginning of the step, and therefore the controlling ion. It provides a better fit in the film-controlled experiments. For simulation purposes the free diffusion coefficient of hydrogen ion, $D^f_H = 9.31 \times 10^{-9}$ m^2/s, has been used.

The general trend of the response curves with the mentioned parameters is shown in Figures 4 and 5. The curves show a similar general form: as L and Nu increase, the elution kinetics are faster, and the same can be said when C_{si} decreases. From Figures 4 and 5, two important conclusions may be drawn. First, a significant change in L, which can only be reached by changing the flow rate (R_p can only be varied in a narrow range for commercial resins), affects markedly the first part of the curves. The relation C/C_0 reaches very low values at very short times. It would mean that the time available for the experimental measurements would be very limited. For $L = 5000$ and $D_i/R_p^2 = 7.5 \times 10^{-3}$ s^{-1}, as an example, in only 10−11 s a value of $C/C_0 = 0.01$ (near the limit of detection of the analyzer depending on the system) would be reached. Therefore, that fact should be taken into account in order to select experimental conditions that permit reliable measurements. Second, for low solution concentrations or small

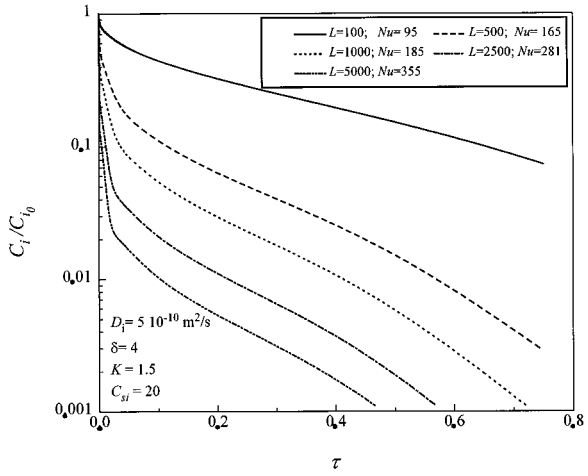

Figure 4. Theoretical desorption curves, C_i/C_{i_0} vs τ, calculated from the ZLC model. Influence of the kinetic parameters, L and N. ($D_i = 5 \times 10^{-10}$ m^2/s, $\delta = 4$, $K = 1.5$, $C_{si} = 20$.)

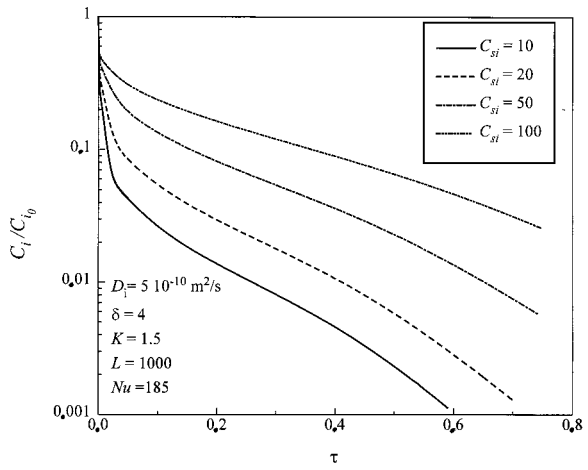

Figure 5. Theoretical desorption curves, C_i/C_{i_0} vs τ, calculated from the ZLC model. Influence of the capacity parameter, C_{si}. ($D_i = 5 \times 10^{-10}$ m^2/s, $\delta = 4$, $K = 1.5$, $L = 1000$, $Nu = 185$.)

values of the flow rate, the process can be film diffusion controlled. Figure 6 shows the concentration profiles inside the particle in different conditions. For low values of L or high values of C_{si} the slope of the profiles inside the particle is small, even at short times. Although the effect of film diffusion has been taken into account in the model, it will be desirable to work far from film diffusion control conditions. Helfferich's criteria can help to elucidate the controlling mechanism of the process (Helfferich, 1962).

Experimental Section

The experimental system is shown schematically in Figure 7. Two metering peristaltic pumps (Watson-Marlow 505S; maximum flow 4 mL/s), previously calibrated, were used to provide streams of ion solutions at constant flow rates. The switch valve was a standard four-port valve, and the detector was a conductivity meter Crison 2201. The ZLC column was placed between the switch valve and the conductivity cell. It was a small filter holder of 2.5 cm i.d., with a shallow bed of resin (2 mm, bed volume = 0.98 mL). The volume of the cell was 3.5 mL, and the volume of the tubing between the valve and the conductivity cell was approximately equal to 3.2 mL. The porosity of the cell, ϵ, was equal to 0.8 and the porosity of the resin bed, ϵ_b, used in eqs 26 and 27 was 0.31. The connections of the ZLC with the four-port valve and conductivity cell were made as close as possible in order to minimize the extra column holdup. Conductivity data were recorded continuously by a computer.

Table 1. Properties of Amberlite IR-120

matrix type	Geliform
functional structure	sulfonic
moisture content (%)	47−62
average particle diameter (cm)	0.055
particle density (g of dry resin/cm^3 of wet resin)	0.560
total exchange capacity (mequiv/g of dry)	5.05

Table 2. Ion Diffusivities and Separation Factors

species	D^f [a] (m^2/s)	K^b
H^+	9.31×10^{-9}	
Na^+	1.33×10^{-9}	1.70
K^+	1.96×10^{-10}	2.45

[a] Values from Slater (1991). [b] Values from de Lucas et al. (1992).

Initially, a shallow sample of resin (2 mm) was placed in the ZLC cell and a solution was continuously fed, until resin saturation. At zero time a solution containing a different counterion and the same total concentration was fed at sufficiently high flow rate, and the desorption curve was analyzed in terms of the concentration of the ion initially in the resin phase versus time. Once the resin is completely saturated with the entering counterion, the reversal elution curve was carried out, returning the resin sample to the primitive state. All the experiments were carried out at 25 °C.

Each run was conducted twice, showing good reliability. Experimental measurements demonstrated that the volume of resin in the ZLC was enough to obtain sufficient sensitivity to follow the tails of desorption curves with accuracy.

The systems under study were solutions of HCl, NaCl, and KCl at two concentrations, 500 and 100 mol/L. The resin was a strong cationic sulfonic type gel, Amberlite IR-120, manufactured by Rohm and Haas. The resin samples were used as supplied by the manufacturer, with no particle size classification attempted. Before their use in experiments the samples were pretreated conventionally by repeated washings with HCl, NaCl, and deionized water. The physical properties of the resin are summarized in Table 1.

Results and Discussion

The Nernst−Planck model requires the knowledge of the resin phase self-diffusivity of each ion involved in the process. Reliable correlations linking resin-phase diffusivity to liquid-phase diffusivity are not available, and the different values proposed in the literature are somewhat contradictory (Slater, 1991).

The experimental desorption curves for the system sodium−hydrogen at $C_{i_0} = 500$ mol/m^3 and different flow rates are shown in Figures 8 and 9, together with the model results. The values of $D_{Na} = 1.35 \times 10^{-10}$ m^2/s and $D_H = 5.6 \times 10^{-10}$ m^2/s were determined from a fit of the experimental data. The free diffusion coefficients of ions and the separation factors used for calculations are shown in Table 2. A good fitting between the experimental data and the computational results was obtained in such conditions. An acceptable range of sensitivity (until $C/C_0 = 0.001$) of the analyzer was available for the measurements.

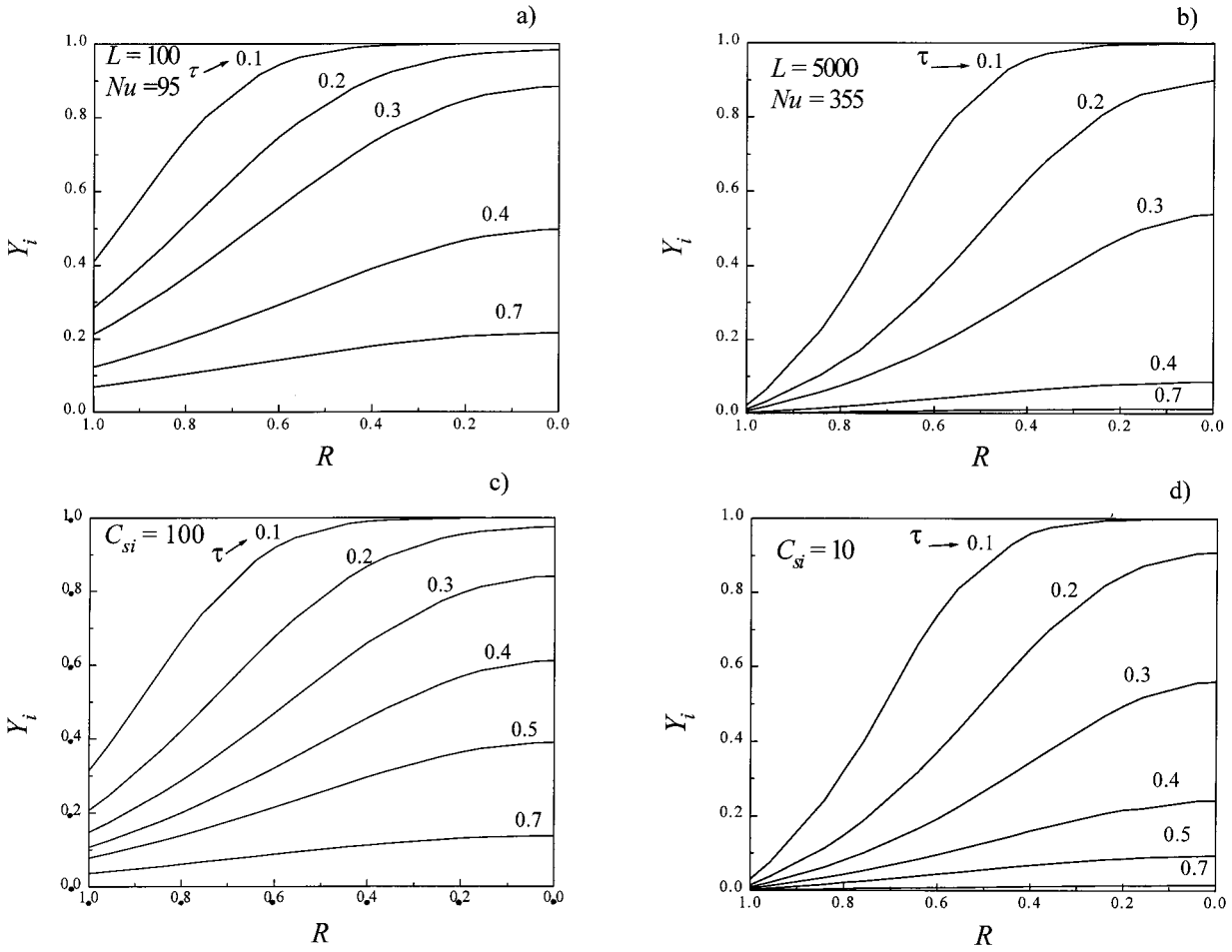

Figure 6. Evolution of the dimensionless radial concentration profiles, Y_i vs R, inside the particle calculated from the ZLC model. Influence of the kinetic parameters, L and Nu: (a) $L = 100$, $Nu = 95$, $C_{si} = 20$; (b) $L = 5000$, $Nu = 355$, $C_{si} = 20$. Influence of the capacity parameter, C_{si}. (c) $L = 1000$, $Nu = 185$, $C_{si} = 100$; (d) $L = 1000$, $Nu = 185$, $C_{si} = 10$. ($D_i = 5 \times 10^{-10}$ m^2/s, $\delta = 4$, $K = 1.5$.)

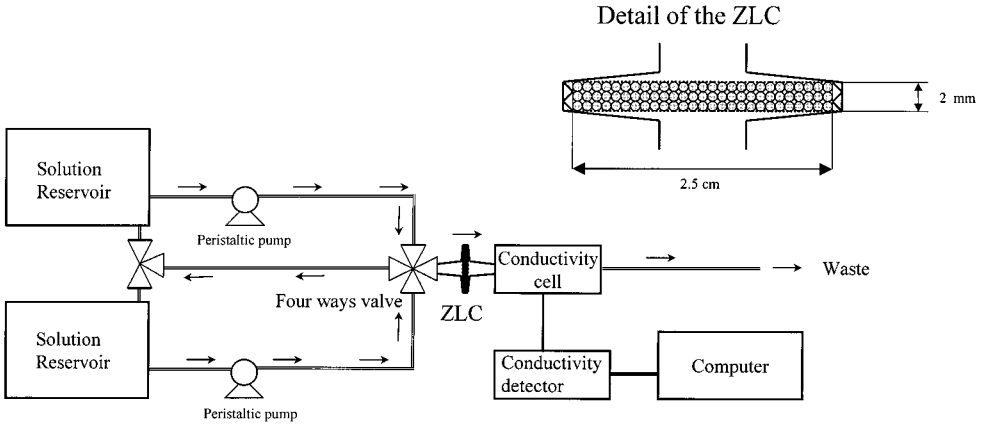

Figure 7. Schematic diagram of the experimental system.

Figure 10 shows the comparison between the elution Na−H and the reversal H−Na, in the same conditions. The asymmetrical behavior of desorption, as predicted by the Nernst−Planck model, can be seen. The main features of the curves can be easily explained based on the computational work. When Na^+ is initially in the resin, the unfavorable equilibrium slows down the release of the Na^+ and the concentration decreases more sharply than when the hydrogen ion is initially in the resin. In the long time region, it can be seen that the exchange rate increases when H^+ is in the resin and decreases when Na^+ is the ion initially in the resin; namely, at the end the interdiffusion coefficients tend to that of the minority ion in the resin.

A greater difference between the reversal curves might be expected because a large value δ is being used. Nevertheless, equilibrium is acting in an opposite direction to the relation of diffusivities. If H^+ is initially in the resin ($K > 1$), the ion exchange prefers the species in solution and the rate of exchange is faster; when Na^+ is initially in the resin ($K < 1$), the rate of exchange is slower.

The experimental desorption curves for the system potassium−hydrogen are shown in Figures 11 and 12,

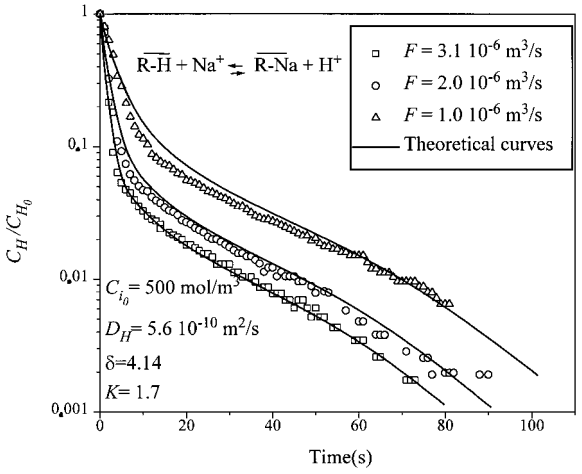

Figure 8. Semilog plot of C_H/C_{H_0} vs time in the ZLC system. System H−Na. Influence of flow rate on desorption curves. C_0 = 500 mol/m^3.

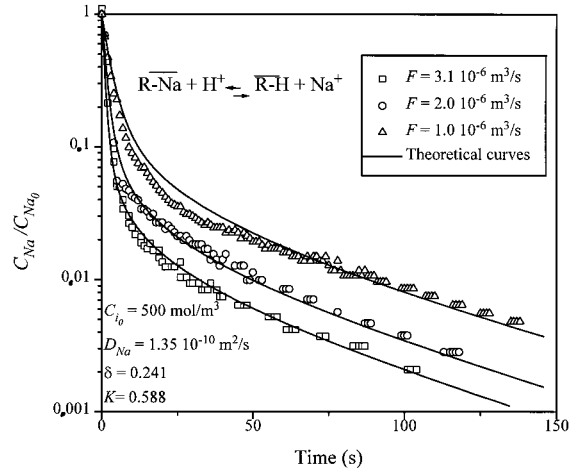

Figure 9. Semilog plot of C_{Na}/C_{Na_0} vs time in the ZLC system. System Na−H. Influence of flow rate on desorption curves. C_{i_0} = 500 mol/m^3.

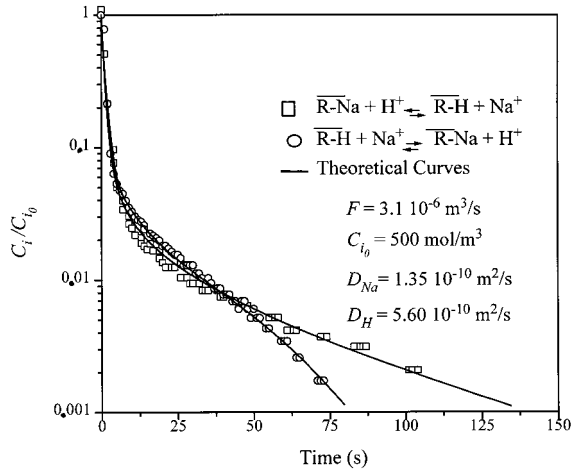

Figure 10. Semilog plot of C/C_0 vs time in the ZLC system. Comparison between the reversal elution curves for the system sodium−hydrogen. C_{i_0} = 500 mol/m^3.

together with the model results. With a fixed value of the intraparticle self-diffusivity of the H^+ ion, only the self-diffusion coefficient of K^+ could be fitted. A value of D_K =1.92 × 10^{-10} m^2/s, a bit greater than the sodium self-diffusion coefficient, was obtained. These results are in good agreement with the relation between the

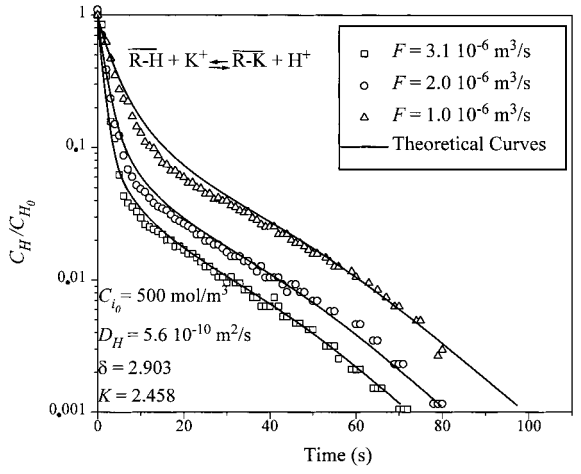

Figure 11. Semilog plot of C_H/C_{H_0} vs time in the ZLC system. System H−K. Influence of flow rate on desorption curves. C_{i_0} = 500 mol/m^3.

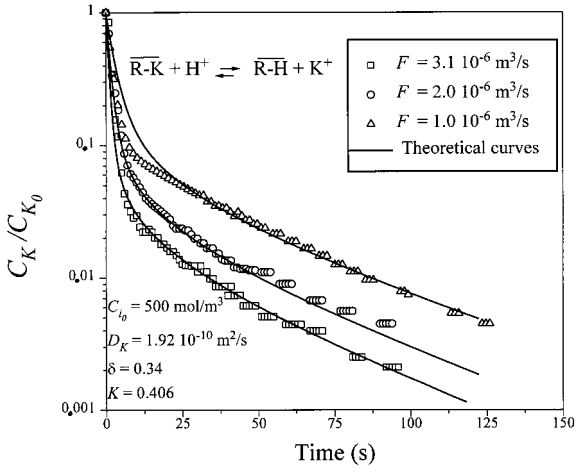

Figure 12. Semilog plot of C_K/C_{K_0} vs time in the ZLC system. System K−H. Influence of flow rate on desorption curves. C_{i_0} = 500 mol/m^3.

free diffusion coefficients of both ions and the values reported in the literature (Fernández et al., 1994). Table 3 shows a comparison between the values obtained in the present work and the different values reported in the literature. The present values are in order of magnitude similar to those previously reported, even showing a complete agreement with some values obtained for similar types of resins.

The systems K−Na and Na−K at C_{i_0} = 500 mol/L could not be investigated because the range of sensitivity of the analyzer in those conditions was too narrow to obtain any meaningful results. Nevertheless, to investigate the accuracy of the self-diffusion coefficients obtained previously, a series of experiments were carried out at C_{i_0} = 100 mol/L, for the mentioned system. Although the proposed model includes an equation to consider the film mass-transfer resistance, Hellferich's criteria was used to estimate which was the controlling resistance at that concentration:

$$\frac{QD_{ij}}{C_T K_L R_p}(5 + 2K) << 1 \qquad \text{particle diffusion control} \tag{28}$$

$$\frac{QD_{ij}}{C_T K_L R_p}(5 + 2K) >> 1 \qquad \text{film diffusion control} \tag{29}$$

Table 3. Summary of Effective Diffusion Coefficients for H, Na, and K in Different Ion Exchangers

species	ion exchanger	DVB (%)	D_i (m²/s)	ref
H^+	Zeo-Karb 225	8	5.59×10^{-10}	Turner et al. (1966)
H^+	Dowex 50WX12	12	8.67×10^{-10}	Goto et al. (1981)
H^+	Dowex 50WX8	8	2.42×10^{-9}	Yoshida and Kataoka (1987)
H^+	Amberlite IR-120	8	2.3×10^{-10}	Melis et al. (1996)
Na^+	Zeo-Karb 225	8	1.21×10^{-10}	Turner et al. (1966)
Na^+	Diaion SK1B		1.35×10^{-10}	Kataoka et al. (1973)
Na^+	Dowex 50X8	8	2.05×10^{-10}	Gupta et al. (1979)
Na^+	Dowex 50WX12	12	1.29×10^{-10}	Goto et al. (1981)
Na^+	Dowex 50X80	8	1.57×10^{-10}	Graham and Drafnoff (1982)
Na^+	Dowex 50X80	8	1.6×10^{-10}	Yoshida and Kataoka (1987)
Na^+	Dowex 50X10	10	1.1×10^{-10}	Yoshida and Kataoka (1987)
Na^+	Lewatit S100		9×10^{-11}	Fernández et al. (1994)
Na^+	Amberlite IR-120	8	5×10^{-11}	Melis et al. (1996)
K^+	Dowex 50X80	8	1.34×10^{-10}	Boyd and Soldano (1953)
K^+	Lewatit S100		1.28×10^{-10}	Fernández et al. (1994)

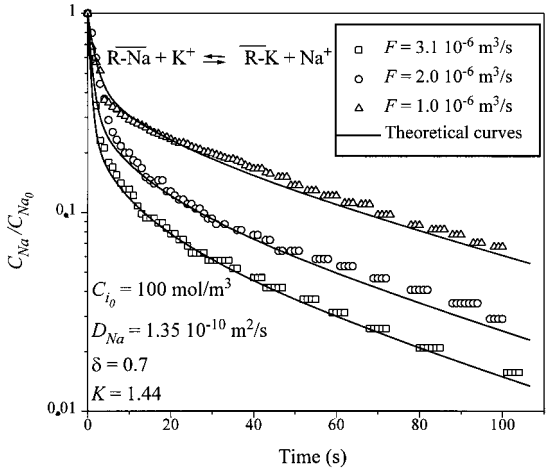

Figure 13. Semilog plot of C_{Na}/C_{Na_0} vs time in the ZLC system. System Na−K. Influence of flow rate on desorption curves. C_{i_0} = 100 mol/m³

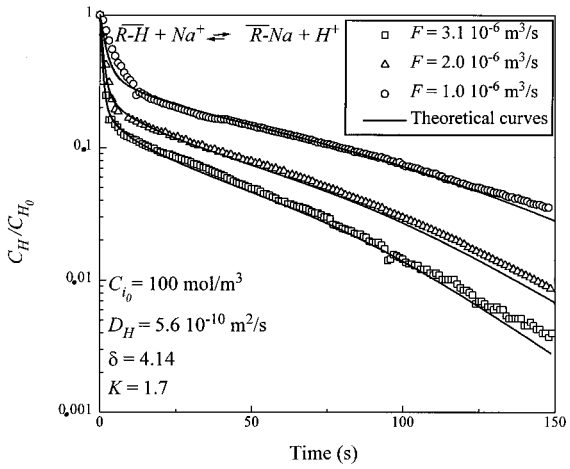

Figure 14. Semilog plot of C_H/C_{H_0} vs time in the ZLC system. System H−Na. Influence of flow rate on desorption curves. C_{i_0} = 100 mol/m³.

An average value between the intraparticle self-diffusion coefficients of the involved ions was used to evaluate Helfferich's criteria. Values ranging between 0.95 and 1.5 were obtained in both cases. This means that both mechanisms affect the rate of exchange but are not completely externally film diffusion controlled. Figure 13 shows the good fitting between the experimental and the theoretical curves for the system Na−K, confirming the validity of the proposed values and the capacity of the model for the prediction of the experimental results in a wide range of conditions.

Finally, a series of experiments for the system Na−H and K−H were carried out at C_{i_0} = 100 mol/m³. As an example, the elution curves for the system H−Na are shown in Figure 14. Those experiments are clearly film diffusion controlled when the ion H^+ is initially in the resin. Helfferich's criteria takes values between 2.76 and 4.03 for the system H−Na. The quasi-linear response of the system confirms that the film diffusion is the controlling step in that case.

Conclusions

A mathematical model for analyzing ZLC desorption curves in binary ion exchange systems has been developed. The influence of the parameters affecting the response of the system has been analyzed.

Intraparticle diffusivities of Na^+, K^+, and H^+ have been obtained using this experimental procedure. The values obtained are of the same order of magnitude as those previously reported in the literature. The capability of the proposed model to simulate the performance of the system in a wide range of conditions has been demonstrated.

The ZLC method can therefore be useful for the measurement of effective self-diffusion coefficients in ion exchangers.

Acknowledgment

J.F.R. acknowledges financial support of his stay in the LSRE of Porto from the rectorship of the University of Castilla−La Mancha.

Nomenclature

C_i = concentration of species i, mol/m³
C_{si} = capacity parameter, eq 22
C_T = total ionic concentration in solution, mol/m³
D_i = intraparticle diffusion coefficient of species i, m²/s
D^f = free diffussion coefficient of the species, m²/s
D_{ij} = interdiffusion coefficient, eq 7, m²/s
F = Faraday constant
F = flow rate, m³/s
K_L = film mass transfer coefficient, m/s
K = isotherm constant separation factor
L = dimensionless parameter of ZLC, eq 24
Nu = Nusselt number, eq 22
q_i = solid-phase concentration of species i, mol/m³
Q = total solid-phase capacity, mol/m³
r = spacial coordinate in the particle, m
R = dimensionless spacial coordinate in the particle
Re = Reynolds number, eq 27
R = perfect gas constant

Sc = Schmidt number, eq 27
t = time, s
T = temperature
u = superficial velocity, m/s
V = volume of the cell, m^3
X_i = dimensionless concentration of species i in the fluid phase
Y_i = dimensionless concentration in the resin phase

Greek Symbols

δ = ratio between the diffusivities of ions i and j
ϵ = void fraction of the cell
ϵ_b = bed porosity
ϕ = electric potential
μ = fluid viscosity, kg/m s
ρ = fluid density, kg/m^3
τ = dimensionless time

Literature Cited

Boyd, G. E.; Soldano, B. A. Self-diffusion of Cations in and through Sulfonated Polystyrene Cation-exchange Polymers. *J. Am. Chem. Soc.* **1953**, *75*, 6091.

Brandani, S.; Ruthven, D. M. Analysis of ZLC Desorption Curves for Liquid Systems. *Chem. Eng. Sci.* **1995**, *13*, 2055.

Brandani, S.; Ruthven, D. M. Analysis of ZLC Desorption Curves for Gaseous Systems. *Adsorption* **1996**, *2*, 133.

Chowdiah, V.; Foutch, G. L. A Kinetic Model for Cationic-Exchange-Resin Regeneration. *Ind. Eng. Chem. Res.* **1995**, *34*, 4040.

de Lucas, A.; Zarca, J.; Cañizares, P. Ion-Exchange Equilibrium of Ca^+, Mg^+, K^+, Na^+, and H^+ on Amberlite IR-120: Experimental Determination and Theoretical Prediction of the Ternary and Quaternary Equilibrium Data. *Sep. Sci. Technol.* **1992**, *6*, 843.

Eic, M.; Ruthven, D. M. A New Experimental Technique for Measurement of Intracrystaline Diffusivity. *Zeolites* **1988**, *8*, 41.

Fernández, A.; Rendueles, M.; Rodrigues, A. E.; Díaz, M. Co-Ion Behavior at High Concentration Cationic Ion Exchange. *Ind. Eng. Chem. Res.* **1994**, *33*, 2789.

Finlayson, B. A. *Nonlinear Analysis in Chemical Engineering*; McGraw-Hill: New York, 1980.

Goto, M.; Goto, S.; Teshima, H. Simplified Evaluations of Mass Transfer Resistances from Batch-wise Adsorption and Ion Exchange Data. 2. Nonlinear Isotherms. *Ind. Eng. Chem. Fundam.* **1981**, *4*, 371.

Graham, E. E.; Dranoff, J. S. Application of the Stefan−Maxwell Equations to Diffusion in Ion Exchangers. 2. Experimental Results. *Ind. Eng. Chem. Fundam.* **1982**, *4*, 365.

Gupta, A. K.; Gopala Rao, M.; Mann, R. S. Isotopic Ion-Exchange Studies in Heteroionic Systems. *Chem. Eng. Sci.* **1979**, *34*, 279.

Helfferich, F. *Ion Exchange*; McGraw-Hill: New York, 1962.

Helfferich, F. Model and Physical Reality in Ion Exchange Kinetics. *React. Polym.* **1990**, *13*, 191.

Kataoka, T.; Yoshida, H.; Yamada, T. Liquid-Phase Mass Transfer in Ion Exchange Based on the Hydraulic Radius Model. *J. Chem. Eng. Jpn.* **1973**, *2*, 172.

Kraaijeveld, G.; Wesselingh, J. A. The kinetics of Film-Diffusion-Limited Ion Exchange. *Chem. Eng. Sci.* **1993**, *3*, 467.

Marquardt, D. W. An algorithm for least-squares estimation of nonlinear parameters. *J. Soc. Ind. Appl. Math.* **1963**, *2*, 431.

Melis, S.; Markos, J.; Cao, G.; Morbidelli, M. Separation between Amino Acids and Inorganic Ions through Ion Exchange: Development of a Lumped Model. *Ind. Eng. Chem. Res.* **1996**, *35*, 3629.

Rendueles de la Vega, M.; Loureiro, J. M.; Rodrigues, A. E. Equivalence Between Nernst−Planck and "Corrected" Fick's Law in Modeling Fixed-Bed Ion Exchange Processes. *Chem. Eng. J.* **1996**, *61*, 123.

Rodrigues, A. E.; Beira, E. C. Staged Approach of Percolation Processes. *AIChE J.* **1979**, *3*, 416.

Ruthven, D. M.; Stapleton, P. Measurements of Liquid-Phase Counter-Diffusion in Zeolite Crystals by the ZLC Method. *Chem. Eng. Sci.* **1993**, *1*, 89.

Silva, J. A. C.; Rodrigues, A. E. Sorption and Diffusion of *n*-Pentane in Pellets of 5-A Zeolite. *Ind. Eng. Chem. Res.* **1997**, *36*, 493.

Slater, M. J. *The principles of ion exchange technology;* Butterworth−Heinemann: Oxford, U.K., 1991.

Turner, J. C. R.; Church, M. R.; Johnson, A. S. W.; Snowdon, C. An Experimental Verification of the Nernst−Planck Model for Diffusion in an Ion-Exchange Resin. *Chem. Eng. Sci.* **1966**, *21*, 317.

Yoshida, H.; Kataoka, T. Intrapaticle Ion-Exchange Mass Transfer in Ternary System. *Ind. Eng. Chem. Res.* **1987**, *26*, 1179.

Received for review September 22, 1997
Revised manuscript received February 13, 1998
Accepted February 23, 1998

IE970684S